

# An analysis of the J-method from the perspective of the AGB evolution

C. Gavetti<sup>1,2</sup>, P. Ventura<sup>2</sup>, F. Dell'Agli<sup>2</sup>, M. Correnti<sup>2,3</sup>, F. La Franca<sup>1</sup>

<sup>1</sup> Dipartimento di Matematica e Fisica, Università degli Studi Roma Tre, via della Vasca Navale 84, 00100, Roma, Italy

<sup>2</sup> INAF, Observatory of Rome, Via Frascati 33, 00077 Monte Porzio Catone (RM), Italy

<sup>3</sup> ASI-Space Science Data Center, Via del Politecnico, I-00133, Rome, Italy

Received September 15, 1996; accepted March 16, 1997

## ABSTRACT

**Context.** The JAGB method has been proposed over the last years as a possible distance indicator for the galaxies in the Local Group and possibly beyond. The nature of the stars populating the J region, as also the conditions on the star formation history and on the structural properties of the galaxies for the straight application of this method need still to be investigated.

**Aims.** We study the populations of the J region of the colour-magnitude ( $J - K, J$ ) plane of the Large and Small Magellanic Cloud (LMC and SMC, respectively), to relate the shape of the J luminosity function (JLF) to the details of the formation histories of the two galaxies, in the attempt of distinguishing the general aspects of the JLF to those more sensitive to the stellar population of the specific galaxy considered.

**Methods.** We use a population synthesis approach, based on the combined results from stellar evolution and dust formation modelling, to find the expected distribution of the stars within the J region, and compare it with that derived from the observations of LMC and SMC stars. Some physical assumptions, mostly related to the modelling of the red giant branch and asymptotic giant branch phases of stars, are tuned, until satisfactory agreement between the expectations from synthetic modelling and the observational evidence is reached.

**Results.** The sources observed within the J region are identified with stars that have recently reached the C-star stage, and have not yet accumulated the extremely large amounts of carbon required to make the evolutionary track to evolve off the J region. Generally speaking,  $2 - 3 M_{\odot}$  stars stay longer within the J region, while lower mass objects evolve there for at most a couple of inter-pulse phases. The analysis of the JLF of the LMC, peaked at the J magnitudes expected for these stars, confirm this understanding. In the SMC the distribution of the J fluxes is shifted to higher J magnitudes when compared to the LMC, which we interpret as the signature of an average older population, with smaller mass progenitors.

**Key words.** stars: AGB and post-AGB – stars: abundances – stars: evolution – stars: mass-loss

## 1. Introduction

During the past decades, increasing attention has been devoted to the asymptotic giant branch (AGB), the evolutionary phase experienced by all stars with initial mass between  $1$  and  $8 M_{\odot}$ , which begins after the consumption of central helium, and extends until the external envelope of the star is lost. AGB stars are often split into different sub-classes, such as those that haven't experienced any thermal pulse yet (early-AGB), those enriched in carbon in the surface regions (carbon stars), or those surrounded by dust. An example of the distinction among AGB stars is found in Weinberg & Nikolaev (2001). During the AGB phase the stars lose their envelopes, enriching the surrounding medium with chemically processed gas (Kobayashi et al. 2020; Romano 2022). These ejecta play a key role in the production of carbon and nitrogen (Vincenzo et al. 2016), in shaping the chemical patterns of Local Group star-forming regions, and possibly in the origin of multiple stellar populations in globular clusters (Ventura et al. 2001).

AGB stars are also among the most efficient dust producers, as their circumstellar envelopes provide ideal conditions for grain condensation (Gail & Sedlmayr 1985). Together with supernovae, they dominate the cosmic dust budget, although their relative contributions remain debated (Schneider & Maiolino 2023). Understanding AGB dust formation is thus essential both

for computing stellar dust yields and for interpreting IR observations, given the reprocessing of stellar radiation by circumstellar dust.

Modern AGB models now include self-consistent treatments of dust formation in stellar winds (Ventura et al. 2012, 2014; Nanni et al. 2013, 2014), following the approach of the Heidelberg group (Ferrarotti & Gail 2001, 2002, 2006), which predict dust composition, quantity and production rates. These models have been widely applied to estimate the AGB dust budget in nearby galaxies (Schneider et al. 2014) and to interpret evolved stellar populations in the Magellanic Clouds (MCs) and other Local Group systems (Dell'Agli et al. 2014b, 2015a,b; Nanni et al. 2016, 2019; Dell'Agli et al. 2016, 2018, 2019; Gavetti et al. 2025).

The capability to investigate the evolved stellar populations of galaxies is becoming increasingly relevant in the James Webb Space Telescope (JWST) era. Due to its unprecedented infrared sensitivity, JWST enables the detection of resolved stellar populations in galaxies well beyond the Local Group and provides an exceptional tool for studying AGB stars (Correnti et al. 2025; Bortolini et al. 2025). For a significant fraction of these systems, AGB stars represent important tracers for reconstructing their star formation histories (SFHs), due to their age sensitivity in the NIR (Lee et al. 2024b; Bortolini et al. 2024).

A further motivation to study the structure, evolution and dust formation of AGB stars is their potential use as distance indicators. This idea originates from Nikolaev & Weinberg (2000), who identified a region in the  $(J - K_s, K_s)$  plane of the LMC - later called "J region" - dominated by carbon stars and proposed them as standard candles to trace the 3D structure of the LMC. Subsequent works (Madore & Freedman 2020; Freedman & Madore 2020) extended this approach to nearby galaxies, coining the JAGB method, and found that stars within  $1.3 < J - K < 2.0$  mag have a mean  $M_J \sim -6.20$  mag. However, Ripoche et al. (2020) reported systematic differences between LMC, SMC and Milky Way, suggesting a possible metallicity dependence. More recently, Magnus et al. (2024) refined the calibration using Gaia data, selecting a clean carbon star sample within  $1.5 < J - K < 2.0$  mag and a 1.2 mag wide J window. They confirmed a mean  $M_J$  of  $\sim -6.25$  mag for the LMC and  $\sim -6.18$  mag for the SMC.

The results discussed above highlight the need for a precise calibration of the JAGB method to enable its use for measuring distances to more distant galaxies. Indeed, JAGB stars are, on average, significantly brighter than the tip of the red giant branch (TRGB), allowing distance determinations well beyond the TRGB limit. Compared to Cepheids, the JAGB method requires only a single epoch of observations and can be applied to galaxies hosting stellar populations aged between  $\sim 200$  Myr and 1 Gyr, whereas Cepheids are confined to the disks of spiral and irregular systems. These advantages, together with the advent of JWST, have motivated the community to apply this technique to an increasing number of galaxies to refine the determination of the Hubble constant (Lee et al. 2024a; Li et al. 2025; Freedman et al. 2025).

Against this background, we decided to start a new research project, designed to understand if and under which conditions the JAGB method can be safely used to determine the distance of galaxies, based on the study of the evolution of the positions of the stars on the CMD, as they evolve through the AGB. To this aim we consider AGB models of different mass and chemical composition, where dust formation is taken into account, to allow the variation of the spectral energy distribution (SED) to be followed, then the determination of the IR colours and magnitudes. We concentrate on the evolutionary phases during which the stars evolve across the J region, defined according to the recommendations by Magnus et al. (2024), to clarify the following points: a) which stars enter the J region?; b) which is the duration of the stay of the stars within the J region?; c) which is the chemical composition, the dust mineralogy and the dust production rate (DPR) of the stars during these evolutionary phases? Answering these questions is the sine qua non condition for a general application of the J method to measure distances of galaxies.

In this first work we describe the main factors affecting the crossing and the time of stay of AGB stars in the J region, in relation to the mass and the formation epoch of the stars. We start by analysing the LMC and the SMC, since for these two galaxies both the SFH and the age-metallicity relationship (AMR) are robustly known, which makes the comparison between theoretical modelling and observations easier. We compare the J luminosity function of the stars in the J region of the CMDs of the LMC and SMC published in Magnus et al. (2024), with results based on a population synthesis approach, which relies on the modelling of the AGB evolution and the dust formation process. The goal of the present analysis, other than confirming the possibility of reproducing the observed luminosity functions, is the characterisation of the LMC and SMC stars nowadays populating the J region, in relation to the mass, chemical composition and formation epoch of the progenitors.

This work is to be considered as a first step towards the comprehension of the conditions under which the J method can be reliably applied as a distance indicator, an argument that will be deepened in the following investigations on this topic, where all the galaxies for which the JLJ has been derived will be considered, and a general overview of the results obtained with various SFH and AMR will be presented.

The structure of the paper is as follows: the numerical and physical ingredients used to model the AGB evolution and the dust formation process, and the techniques adopted in the population synthesis approach, are described in section 2; the main physical and chemical properties of AGB stars, and the conditions and timing of their crossing the J region of the colour-magnitude  $(J - K, J)$  plane, are discussed in section 3; section 4 is devoted to the application of the population synthesis approach to study the stellar population of the J region of the LMC, to test the possibility to reproduce the results from Magnus et al. (2024); a comparative analysis between the populations of the J regions of the LMC and SMC, in relation to the difference in the SFH of the two galaxies, is addressed in section 5; finally, the conclusions are given in section 6.

## 2. Physical and numerical input

The analysis presented in this work is based on the comparison between the observed J luminosity function of the stars populating the J region of the LMC and the SMC, selected on the basis of the indications given in Magnus et al. (2024), with the results obtained by a population synthesis approach. In the latter we run numerical simulations, based on the SFH and the AMR of the galaxy considered, to calculate the number of stars nowadays evolving through the JAGB, and the mass and metallicity of the progenitors. For the LMC we adopted the SFH derived by Mazzi et al. (2021), combined with the AMR by Carrera et al. (2008), while for the SMC we followed the SFH and the AMR given by Rubele et al. (2018).

Finding the synthetic distribution of the stars across the CMD demands the knowledge of the evolutionary tracks of the stars evolving across the AGB and the time variation of the position along the track. This is obtained by modelling the evolution of stars of different mass and metallicity, combined with the description of the dust formation, which is required to account for the modification of the SED due to the reprocessing of the radiation by dust grains. For this work we used extant evolutionary sequences previously published by our group, of metallicity  $Z = 0.001$  (Ventura et al. 2014),  $Z = 0.004$  and  $Z = 0.008$  (Marini et al. 2021). The above computations were recently extended until the start of the white dwarf cooling, as described in Kamath et al. (2023). For the stars of initial mass  $M \leq 2 M_\odot$ , the computations are first evolved from the pre-MS through the core hydrogen burning and the red giant branch (RGB) phase, until the TRGB, when the helium flash takes place. The simulations are then re-started from the quiescent core helium burning phase, based on the core masses reached at the TRGB. These stars lose a significant fraction of the mass of their envelope during the evolution along the red giant branch (RGB), thus the mass with which they undergo core helium burning is smaller than the initial mass. We assumed that all the stars of mass below  $1.5 M_\odot$  lose  $0.2 M_\odot$  during the ascent along the RGB. In the following we will refer to the mass of these stars at the start of the core helium burning phase, keeping in mind that the mass of the progenitors was  $0.2 M_\odot$  higher. We will test how this choice affects the results obtained.

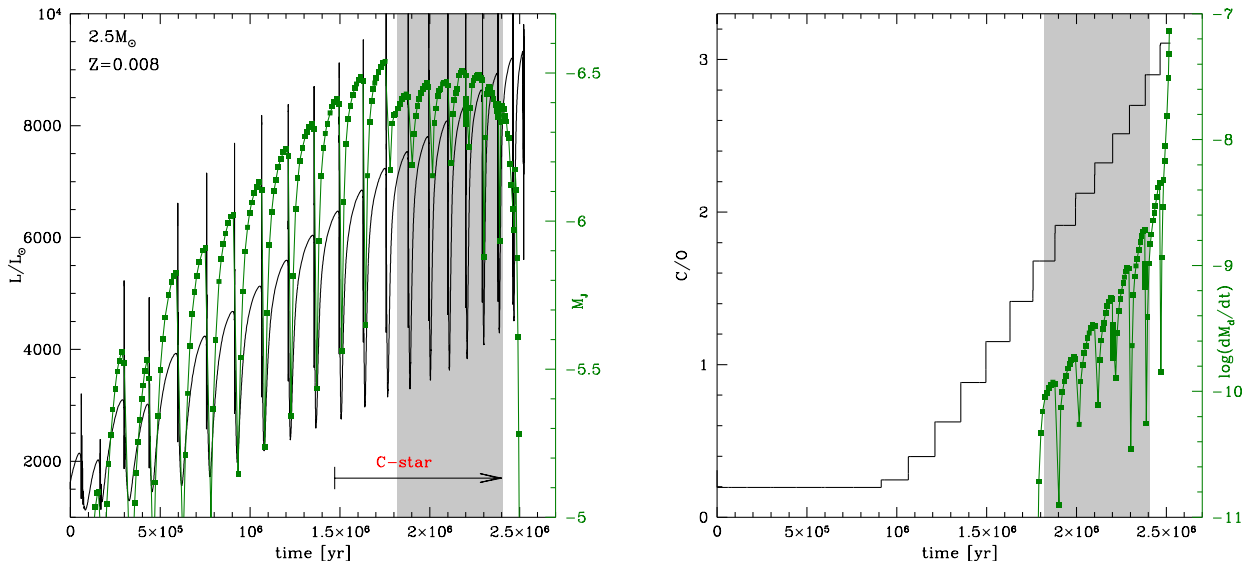


**Fig. 1. Left:** Time variation of the luminosity (black line, scale on the left) and the J magnitude (green, scale on the right) of a model star of initial mass  $2.5 M_{\odot}$  and metallicity  $Z = 0.008$ . The black arrow indicates the start of the C-star phase. **Right:** Time evolution of the surface C/O and the DPR of the same model star shown in the left panel. Times are counted since the beginning of the TP-AGB phase. Grey-shaded regions indicate the phase during which  $1.5 < J - K < 2$  mag.

Dust formation in the wind is described by following the formalism proposed by Ferrarotti & Gail (2006), in the modality extensively described in Ventura et al. (2012). The application of the modelling of dust formation to the results from stellar evolution leads to the determination of the variation of the dust composition and the DPR of the stars as they evolve along the AGB. The final step to build the evolutionary tracks of the stars is the determination of the variation of the SED, which, in turn, is used to find the colours and magnitudes in the selected filters, via convolution of the SED with the corresponding transmission curves. This is done by means of the DUSTY code (Nenкова et al. 1999), which uses as input the results from the modelling of dust formation. This work is based on the sequence of synthetic SEDs recently used by Gavetti et al. (2025).

The evolutionary sequences of the stars of different initial mass and metallicity are available at the CDS. For  $M > 2 M_{\odot}$  stars the masses refer to the initial values, with which the stars formed; for the lower mass counterparts the masses are taken at the start of the core helium burning phase. For each model star we list the variation during the AGB phase of the most relevant physical quantities and of the JHK magnitudes.

### 3. The AGB evolution across the J region

#### 3.1. The main physical aspects of the AGB evolution

The AGB evolution is driven by the gradual growth of the core mass ( $M_C$ ), under the action of the H-burning shell, which for the majority of the AGB lifetime is the unique nuclearly active source in the star (Karakas & Lattanzio 2014). Periodically, helium ignition occurs in a thin shell lying above the degenerate core made up of carbon: because these nuclear episodes occur in conditions of thermal instability (Schwarzschild & Härm 1965), the common terminology used to refer to them is thermal pulse (TP). The rise in the core mass favours the increase in the luminosity, given the approximately linear relationship connecting the two quantities, originally derived by Paczyński (1970), to which all AGB stars obey, with some exceptions that will be discussed later in this section. This behaviour can be seen in the

left panels of Fig. 1 and Fig. 2, which report the AGB evolution of model stars of initial mass  $2.5 M_{\odot}$  and  $4 M_{\odot}$ , respectively. In the  $2.5 M_{\odot}$  case the luminosity increases during the AGB phase from  $\sim 2 \times 10^3 L_{\odot}$  to  $\sim 9 \times 10^3 L_{\odot}$ , while the core mass changes from  $0.52 M_{\odot}$  to  $0.62 M_{\odot}$ . As for the  $4 M_{\odot}$  model star, the luminosity varies from  $\sim 1.2 \times 10^4 L_{\odot}$  to  $\sim 3.5 \times 10^4 L_{\odot}$ , with the core mass increasing from  $0.82 M_{\odot}$ , at the occurrence of the first TP, to  $0.88 M_{\odot}$ , at the end of the AGB.

#### 3.2. The surface chemical composition of AGB stars

The surface chemical composition of AGB stars can be altered by two mechanisms, which leave different chemical imprinting. The third dredge-up (TDU) takes place during the evolutionary phases following the ignition of each TP, when the H-burning shell is temporarily extinguished and the surface convection penetrates inwards until reaching regions of the star previously processed by helium nucleosynthesis (Iben 1974). The primary effect of the TDU is the increase in the surface abundance of carbon, which can lead to the formation of a carbon star. The alternative mechanism able to change the surface chemical composition of AGB stars is hot bottom burning (HBB), which consists in the activation of proton capture nucleosynthesis at the base of the convective envelope, when the temperatures in those regions of the star reach (and exceed) 30 MK (Sackmann & Boothroyd 1992). The ignition of HBB leads to a fast increase in the stellar luminosity (Ventura & D'Antona 2005), with significant deviations from the linear  $M_C - L$  trend found by Paczyński (1970). The impact of HBB on the behaviour of the luminosity can be seen in the left panel of Fig. 2, which shows that the luminosity of the  $4 M_{\odot}$  model star first increases, until  $\sim 3.5 \times 10^4 L_{\odot}$ , then decreases during the final evolutionary phases, because HBB is progressively turned off by the gradual loss of the envelope. This behaviour, typical of the stars experiencing HBB, is not seen in the time variation of the luminosity of the  $2.5 M_{\odot}$  model star shown in Fig. 1, because the ignition of HBB requires core masses in excess of  $0.8 M_{\odot}$  (Ventura et al. 2013), which are reached only by stars of initial mass above  $\sim 3 M_{\odot}$ . On the chemical side, HBB changes the surface chemistry of the star

according to the equilibria of the p-capture nucleosynthesis activated. While the degree of the nucleosynthesis experienced is extremely sensitive to the metallicity of the star (Dell'Agli et al. 2018), the depletion of the surface carbon and the parallel synthesis of nitrogen take place in all the cases when HBB is activated. The main effects of TDU and HBB can be seen in the right panels of Fig. 1 and 2. In the former we note the gradual rise in the surface C/O ratio, which under the effects of repeated TDU episodes grows until a final value around 3. After about half of the AGB lifetime, the surface carbon exceeds oxygen and the star reaches the C-star stage (this is indicated by the horizontal arrow in the lower part of the figure). In the right panel of Fig. 2 we see the effects of HBB in the decrease in the surface carbon and the rise in the nitrogen abundance, which start  $\sim 10^5$  yr after the beginning of the AGB phase. During the very final evolutionary phases the surface carbon increases under the action of TDU, while HBB is turned off.

### 3.3. The position of AGB stars on the $(J - K, K)$ plane

Ventura et al. (2022) divided AGB stars in three different groups, according to the modality with which the surface chemistry changes, and consequently on the chemistry and the quantity of dust produced in their wind, and then on the evolution of the SED: I)  $M < 1 M_{\odot}$  stars, whose chemical composition is substantially unchanged during the AGB evolution, because the core mass is too low for the ignition of HBB, and they lose the external mantle, of a few tenths of solar masses, before repeated TDU events can rise the surface carbon significantly; II)  $1 M_{\odot} < M < 3 M_{\odot}$  stars, which become carbon stars, under the effects of TDU; III) massive AGBs descending from  $M > 3 M_{\odot}$  progenitors, whose surface chemistry mainly reflects the effects of HBB<sup>1</sup>.

Group I) is not of interest for the present investigation, because they evolve on the blue side of the CMD, never entering the J region of the plane. The evolution of the stars belonging to group II) is characterised by the gradual increase in the surface carbon, which proceeds until the almost complete loss of the envelope. A prototype of the evolution of these objects is shown in Fig. 1. The variation of the DPR shown in the right panel of Fig. 1 indicates that dust production is negligible during the O-rich phase, while it becomes higher and higher as carbon is accumulated in the surface regions, until reaching values of the order of  $10^{-7} M_{\odot}/\text{yr}$  during the final part of the AGB evolution. The increase in the surface carbon enhances the efficiency of the dust production mechanism for two reasons, related to the thermal reaction of the external regions of the star to the transition from the O-rich to the C-star phase and to the higher number of C-bearing molecules in the external mantle. The first motivation is that the formation of carbon stars was shown to trigger the enhancement of the surface molecular opacities (Marigo 2002), thus leading to the expansion and cooling of the external layers of the star (Ventura & Marigo 2009, 2010), lower surface gravities, then higher mass loss rates. These conditions turn extremely favourable to the condensation of gaseous molecules into solid grains, because the vaporisation process is partly inhibited by the low temperatures, and the larger densities make a higher num-

<sup>1</sup> The mass limits are slightly dependent on the metallicity. As discussed in Kamath et al. (2023), the lower threshold mass required to reach the C-star stage decreases for lower Z's, because the lower oxygen content eases the formation of carbon stars in metal-poor environments. The lower limit in mass for the ignition of HBB is lower the lower Z, given the hotter temperatures at the base of the envelope of metal-poor, massive AGBs (Dell'Agli et al. 2018).

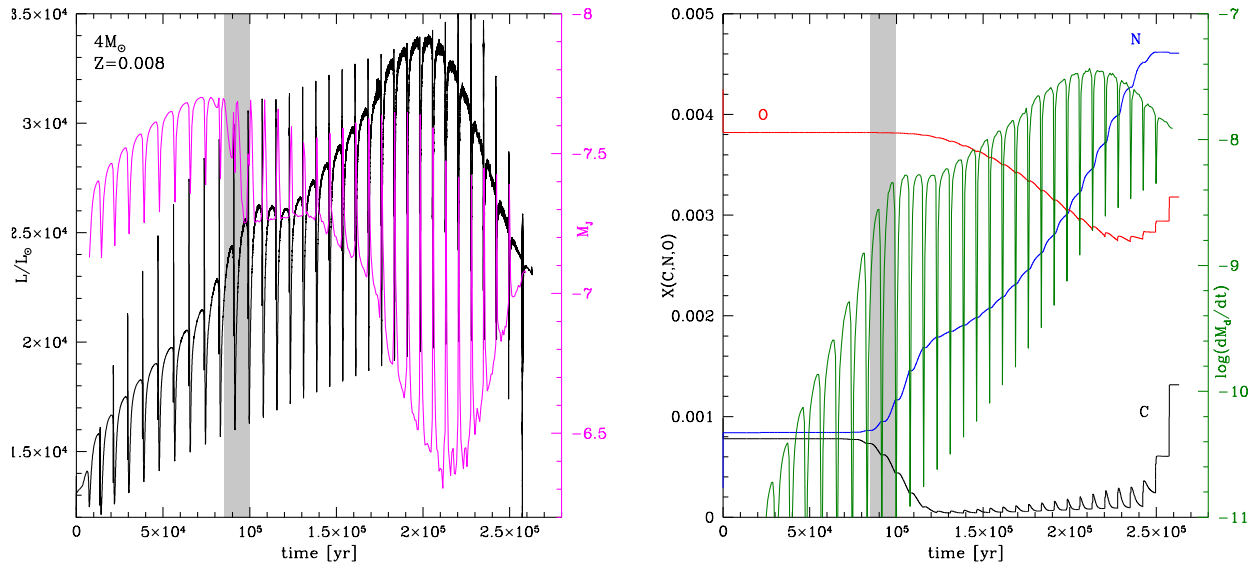
ber of gaseous molecules available to condense into dust grains. A further reason why the higher surface carbon content favours dust production is that the amount of carbon dust formed depends on the carbon excess with respect to oxygen (Ferrarotti & Gail 2006), thus the number of molecules available to form carbon dust is higher the higher the surface carbon. The formation of carbon dust favours the gradual shift of the SED towards the near-IR and then the mid-IR spectral region.

Fig. 3 shows the evolutionary tracks of stars of different initial mass and metallicity  $Z = 8 \times 10^{-3}$  in the CMD. The minimum mass considered in the plot is  $1.1 M_{\odot}$  (which corresponds to a progenitor's mass of  $1.3 M_{\odot}$ ), because the tracks of lower mass stars develop along the blue side of the plane, never turning to the red, thus not crossing the J region, identified with a grey box in the figure. All the evolutionary tracks reported in Fig. 3 correspond to stars belonging to the group II), but the cyan line, corresponding to the  $4 M_{\odot}$  model star. The tracks evolve to the red side of the plane and enter the J region soon after becoming carbon stars.

In the left panel of Fig. 1 we note the  $\sim 0.15$  mag depression in  $M_J$  taking place shortly after the transition to C-star, despite the luminosity of the star increases during the same period: this indicates that the peak of the SED progressively moves to the  $\lambda > 1 \mu\text{m}$  spectral region. In the specific  $2.5 M_{\odot}$  case discussed here the star evolves within the J region of the CMD with  $1.5 < J - K < 2.0$  mag, where it stays for  $\sim 6 \times 10^4$  yr, during 6 interpulse phases following the transition from M type to C-star. The evolutionary track of the  $2.5 M_{\odot}$  model star discussed here is shown in red in Fig. 3. During the very final AGB phases, when the surface C/O exceeds 2.5, the formation of notable quantities of carbon dust favours a significant reprocessing of the radiation released from the photopshere of the star, and the shift of the SED to the mid-IR spectral region. Under these conditions the flux in the J band is almost negligible, so that the evolutionary track moves to the lower far red side of the CMD. We see in Fig. 3 that this behaviour is common to all the stars that become carbon stars, which during the final AGB phases populate the K region of plane, according to the nomenclature adopted by Weinberg & Nikolaev (2001) to identify carbon dust-enshrouded AGB stars on the observational plane. The values of  $M_J$  attained by the star during these advanced evolutionary phases derived from the synthetic modelling are to be taken with some caution; however, this is not an issue for the analysis done here, because these stars do not fall into the J region of the CMD.

These results indicate that  $1 - 3 M_{\odot}$  stars belonging to the group II) introduced earlier in this section evolve into the J region of the CMD when they undergo a transition phase, which starts after becoming carbon stars. The beginning of this phase occurs when the carbonaceous dust in the wind forms with sufficiently large rates, so that the SED is shifted towards the near IR, and  $J - K > 1.5$  mag. The conclusion of this transition time takes place when the excess of carbon with respect to oxygen becomes so large that the dust forms in the wind in quantities large enough to lead to the  $J - K > 2.0$  mag condition. The stars in the J region of the CMD must have accumulated in the surface regions an amount of carbon that corresponds to a specific range of C/O, which in the  $2.5 M_{\odot}$  case discussed here is  $1.7 < \text{C/O} < 2.8$ . We will see that this result cannot be fully generalized, as the exact C/O range for the  $1.5 < J - K < 2.0$  mag condition is sensitive to the mass and the metallicity of the star considered.

Turning to the  $4 M_{\odot}$  model star, whose evolutionary track is reported in cyan in Fig. 3, the results reported in Fig. 2 suggest that massive AGBs evolve into the  $1.5 < J - K < 2.0$  mag region of the plane during the early phases following the ignition of



**Fig. 2. Left:** Time variation of the luminosity (black line, scale on the left) and the J magnitude (magenta, scale on the right) of a model star of initial mass  $4 M_{\odot}$  and metallicity  $Z = 0.008$ . **Right:** Time evolution of the surface carbon (black line), nitrogen (blue), oxygen (red) (black scale on the right) and the DPR (green scale on the right) of the same model star shown in the left panel. Times are counted since the beginning of the TP-AGB phase. Grey-shaded regions indicate the phase during which  $1.5 < J - K < 2$  mag.

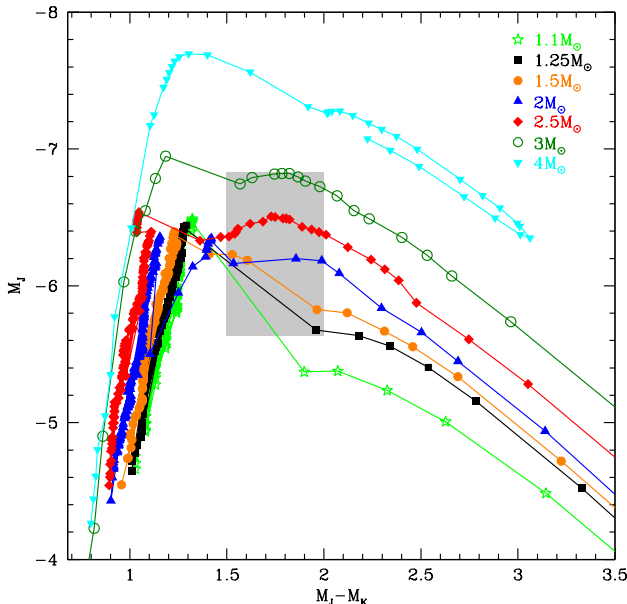


**Fig. 3.** Evolutionary tracks of model stars of metallicity  $Z = 8 \times 10^{-3}$  on the  $(J-K, J)$  colour-magnitude diagram. The different points along the tracks refer to some selected evolutionary stages taken during the AGB phase, chosen in order to well represent the excursion of the tracks on the observational plane. The grey shaded region indicate the box chosen by Magnus et al. (2024) for the J region. The masses given for  $M < 1.5 M_{\odot}$  refer to the values attained at the TRGB.

HBB, when the depletion of the surface carbon and the synthesis of nitrogen begins. During this period the luminosity increases as a reaction to the start of HBB, the star expands and cools, the rate of mass loss increases, so that the circumstellar envelope, for the reasons discussed earlier in this section, becomes an environment favourable for the formation of dust, which in the present case is mostly composed of silicates, with traces of alumina dust (Ferrarotti & Gail 2006; Dell'Agli et al. 2014a; Ventura et al. 2014). This behaviour can be considered as typical

of massive AGBs belonging to the group III) introduced by Ventura et al. (2022), provided that the metallicity is solar or slightly sub-solar, which is the case for the intermediate mass populations of the LMC and SMC.

The results shown in Fig. 2, when compared to those reported in Fig. 1, lead to two important conclusions. First, the time spent by massive AGBs in the  $1.5 < J - K < 2.0$  mag region of the CMD is significantly shorter than for carbon stars (in the specific cases considered here this time is  $\sim 10^4$  yr and  $\sim 6 \times 10^4$  yr for the  $4 M_{\odot}$  and  $2.5 M_{\odot}$  model stars, respectively). An additional important conclusion drawn from inspection of Fig. 1 and Fig. 2 is that the J magnitudes of the stars belonging to the groups II and III) are significantly different when they enter the J region. The inclusion of massive AGBs in the J region of the CMD is sensitive to the choice done for the J extension of the selected box: for instance, it is clear from inspection of Fig. 3 that when the recommended choice proposed by Magnus et al. (2024) is adopted, the  $4 M_{\odot}$  model star considered here would escape detection within the J region.

#### 3.4. The AGB population in the J region of the CMD

The results shown in Fig. 3 indicate that the choice of the size of the box defining the J region proposed by Magnus et al. (2024) is tailored ad hoc to restrict the attention on carbon stars only: indeed this choice rules out massive AGBs, which evolve brighter than the lower J magnitude considered by Magnus et al. (2024), and possible contaminations from low-mass, O-rich stars, which, if present, would evolve to lower J fluxes than the minimum indicated in the aforementioned study.

A deeper inspection of Fig. 3 suggests that the slope of the evolutionary tracks within the J region of the CMD changes with the progenitor's mass: while the J flux of  $M \geq 2 M_{\odot}$  stars keeps constant or even increases during the J phase, the lower mass counterparts are exposed to a more abrupt transition upon becoming carbon stars, which leads to a fast drop in the J flux, such that the evolutionary tracks (see the  $1.1 M_{\odot}$ ,  $1.25 M_{\odot}$  and  $1.5 M_{\odot}$  cases in Fig. 3) cross the J region with a negative slope, pointing the faint, right side of the CMD.

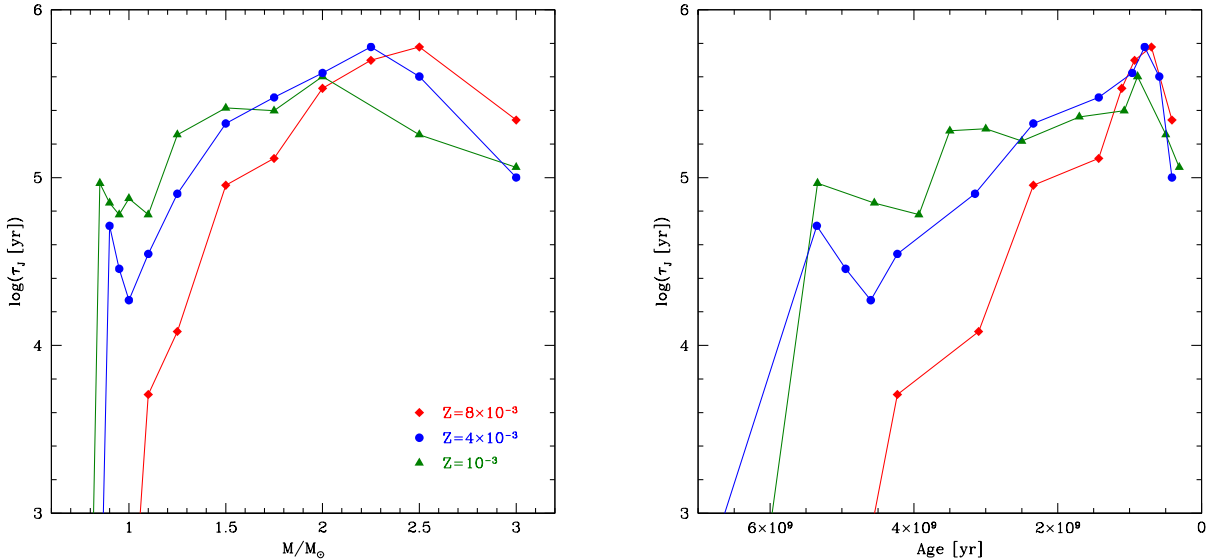


**Fig. 4.** Duration of the evolutionary phase spent by model stars of different metallicity in the box delimiting the J region of the  $(J - K, J)$  plane, according to the definition by Magnus et al. (2024), as a function of the stellar mass (left panel) and age (right). The masses of  $M < 1.5 M_\odot$  stars reported in the abscissa of the left panel refer to the values at the start of the core helium burning phase.

These differences are related to the modality with which the transition from M-type to C-star occurs in stars of different mass.  $M \geq 2 M_\odot$  stars lose little mass during the initial AGB phases when they evolve as O-rich objects, because they are characterised by convective envelopes with masses above  $\sim 1 M_\odot$ , which guarantee a sufficiently large gravitational attraction in the surface regions, which prevents intense mass loss. When reaching the C-star stage, their surface C/O slightly exceeds unity and then grows gradually, because the carbon dredged-up during the chain of TDU events is efficiently diluted with the massive envelope, which prevents dramatic changes in the surface C/O ratio. These objects are expected to populate the J region during different inter-pulse phases, and then to evolve off this zone of the CMD only after a further series of TDU episodes makes C/O to grow bigger than  $\sim 2.5 - 3$ . This is the situation that we encountered earlier in this section when discussing the  $2.5 M_\odot$  model star, whose evolution was shown in Fig. 1. The slope of the evolutionary track within the J regions stems from the balance between the gradual increase in the luminosity, due to the growth of the core mass, and the rise in the surface C/O, which favours carbon dust production, triggering a more and more extended depression of the SED in the J spectral region. Because in these stars the increase in C/O proceeds gradually, the first effects prevails slightly, particularly during the phases immediately after the entrance into the J region, so that the slope of the evolutionary tracks within the J region is positive, or flat.

The stars descending from progenitors of mass below  $2 M_\odot$  evolve differently, because the mass of the envelope is of a few tenths of solar masses when the transition to C-star occurs. This is because, when the AGB phase begins, their envelope is less massive than that of the higher mass counterparts, and this leads to lower surface gravities, which enhances the mass loss rate experienced by the star during the O-rich phase. Under these conditions, the transition to the C-star phase is generally followed by a significant increase in the surface carbon content, because dilution with the gas stored in the external envelope is much less efficient than in the higher mass carbon stars. In these low mass stars the production of carbon dust takes place very efficiently since they become carbon stars: this results into a significant de-

pression of the J flux, and is the reason for the negative slope of the evolutionary tracks in the CMD, as clear in Fig. 3.

From these results we understand that the modality with which the stars enter and evolve into the J region changes notably with the progenitor's mass. The objects of higher mass, in the  $2 - 3 M_\odot$  range, spend in the J region a significant fraction of the time during which they evolve as carbon stars, eventually evolving off that region only after repeated TDU events lifted the surface carbon to quantities that favour efficient dust formation and large IR emission. Conversely, the evolution of the low-mass counterparts within the J region appears more as a real transition phase, as the effects of each TDU event on the surface C/O, hence on the DPR, are more dramatic, so that they easily evolve off the region of the CMD considered.

These arguments regarding the transit of the stars within the J region of the CMD are confirmed by the results shown in Fig. 4, where the duration ( $\tau_J$ ) of the stay in the J region of the stars of different metallicity is shown as a function of the initial mass and the age (left and right panel, respectively). In case of stars with metallicity  $Z = 8 \times 10^{-3}$ , whose evolutionary tracks are shown in Fig. 3, we see in the left panel of Fig. 4 that  $\tau_J$  is positively correlated with the mass of the star and changes from  $\sim 5 \times 10^3$  yr, for  $M = 1.1 M_\odot$ , to  $\sim 6 \times 10^5$  yr, for  $M = 2.5 M_\odot$ . The positive trend of  $\tau_J$  vs mass shows a turning point for the  $3 M_\odot$  model star, because the time scale of the AGB evolution of the latter is shorter than that of the lower mass counterparts. The range of masses considered for the  $Z = 8 \times 10^{-3}$  case is limited to the  $1.1 - 3 M_\odot$  range: this is because the stars that at the TRGB have  $M < 1.1 M_\odot$  never enter the J region, while  $M > 3 M_\odot$  stars evolve to the red side of the plane, but they are too bright with respect to the vertical size of the J box. This limitation indicates that only stars formed between  $\sim 300$  Myr and  $\sim 4$  Gyr ago populate the J region of the CMD, as shown in the right panel of Fig. 4.

The  $\tau_J$  vs mass trends for the  $Z = 10^{-3}$  and  $Z = 4 \times 10^{-3}$  cases shown in Fig. 4 are generally flatter than  $Z = 8 \times 10^{-3}$ , because the C-star condition is reached more easily, owing to the lower content of oxygen, so that the lower mass threshold required for the stars to populate the J region is smaller: we see in Fig. 4

that the minimum mass evolving into the J region is  $0.8 M_{\odot}$  and  $M = 0.9 M_{\odot}$ , for  $Z = 10^{-3}$  and  $Z = 4 \times 10^{-3}$ , respectively.

The variation of  $\tau_J$  with the stellar age, shown in the right panel of Fig. 4, exhibits a behaviour similar to the trend  $\tau_J$  vs mass, given the tight relationship between stellar mass and age. It is clear the importance of the stellar formation that occurred around one Gyr ago for the numerical consistency of the population of the J region of the plane.

#### 4. The J region stellar population of the LMC

We used the methodology described in section 2 to build synthetic distributions of LMC stars on the different observational planes, based on the SFH given in Mazzi et al. (2021) and the AMR by Carrera et al. (2008). The results of this population synthesis analysis in the  $(J - K, K)$  CMD is shown in Fig. 6. We recognize in the distribution of the stars the typical features outlined e.g. by Marigo et al. (2003), and particularly: a) the drop in the K-band luminosity function at  $K \sim 11.9$  mag, where the TRGB is located; b) the cut-off of the oxygen-rich AGB luminosity function at  $K \sim 10.7$  mag; c) the colour gap between the O and C-rich AGB populations, in the  $1.5 < (J - K) < 2.0$  mag region. Most of the carbon stars are found in the  $(J - K) > 1.2$  mag region, although a few C-rich objects are also expected to populate the AGB branch above the TRGB: these are the progeny of  $2 - 3 M_{\odot}$  stars, which during the phases immediately following the start of the C-star phase evolve into the blue region of the CMD (the interested reader can find an exhaustive discussion on this argument in Gavetti et al. in prep.).

For what concerns specifically the J region, it is clear from the arguments presented in the previous section that the numerical consistency and the distribution of the stars within this region of the CMD depends on the number of stars descending from  $\sim 1 - 3 M_{\odot}$  progenitors nowadays evolving through the AGB phase. Therefore, the SFH of the galaxy in the epochs between 300 Myr and 4 Gyr ago is the key factor to be considered, along with the AMR, particularly the metallicity of the interstellar medium in those times. These restrictions are partly sensitive to the criterion adopted to select the J region and hold strictly for that proposed by Magnus et al. (2024). If the J region considered was extended to brighter J fluxes than the limits proposed by Magnus et al. (2024), stars more massive than  $3 M_{\odot}$  would need to be considered, thus even the recent star formation, occurred  $\sim 100 - 200$  Myr ago, should be examined. No significant changes are expected if the chosen box for the J region is extended to fainter magnitudes, since the present choice is such that, as shown in Fig. 3, even the evolutionary tracks of the lowest luminosity carbon stars, i.e. those descending from old, low-mass progenitors, cross the J region of the  $(J - K, J)$  plane; the only exception would be found in the galaxies characterised by the presence of an old, metal-rich stellar population, as under those conditions low-mass, oxygen-rich stars during the final AGB phases produce amounts of silicate sufficiently large to deviate the evolutionary tracks towards the faint side of the  $1.5 < J - K < 2.0$  mag strip of the CMD. However, this is not the case neither for the LMC, nor for the SMC, which will be discussed in next section.

The J luminosity function (JLF) obtained for the LMC by means of the population synthesis method is reported as a black line in the left panel of Fig. 5, while the distribution of the (initial) masses of the stars populating the J region is shown in the right panel of the figure.

Inspection of Fig. 5 shows a satisfactory agreement between the present findings and the results shown in the Fig. F3 in Mag-

nus et al. (2024), particularly for what attains the peak of the distribution at  $M_J = -6.35$  mag and the general shape of the JLF, which drops to half the peak value at  $M_J = -6.55$  mag and  $M_J = -6$  mag on the bright and faint sides of the distribution, respectively. Full consistency is also found for the average J magnitude, which is around  $M_J = -6.25$  mag in both cases.

The mass distribution shown in the right panel of Fig. 5 shows up two peaks, centered at  $1.7 M_{\odot}$  and  $2.5 M_{\odot}$ , related to stars formed during the peaks in the SFH of the LMC occurred 1.5 Gyr and 800 Myr ago (Mazzi et al. 2021), respectively. The older peak in the SFH is higher than the younger one, so that  $1.5 \leq M < 1.8 M_{\odot}$  stars currently evolving along the AGB outnumber by almost a factor two the  $2.2 - 2.7 M_{\odot}$  counterparts. However, this is not the case for the J region, because, as shown in Fig. 4, the latter stars spend a significant fraction of the AGB lifetime within that area of the CMD, thus they provide the dominant contribution to the overall population of the J region: the peak in the JLF at  $M_J = -6.35$  mag, and also the two nearest bins in the distribution, are almost entirely due to the presence of  $\sim 2.5 M_{\odot}$  stars. The asymmetry of the JLF around the peak value is due to the excess of  $1.5 - 2 M_{\odot}$  stars, which provide the dominant contribution to the faint side of the distribution, with respect to  $M > 2.5 M_{\odot}$  stars, which contribute to the bright side of the JLF.

The present analysis indicates that about 2/3 of the stars in the J region of the LMC descend from  $\sim 2.5 M_{\odot}$  progenitors, formed between 700 Myr and 1 Gyr ago. These stars are characterised by surface C/O ratios in the  $1.5 - 3$  range and are producing carbon dust at rates  $\sim 2 - 3 \times 10^{-9} M_{\odot}/\text{yr}$ , distributed between solid carbon dust, which accounts for a fraction of the total dust formed between 50% and 75%, and silicon carbide (SiC), whose contribution is between 25% and 50%. Solid iron and other dust species are formed in minor quantities and do not affect the shape of the SED. The luminosities of these objects are in the  $7000 - 9000 L_{\odot}$  range, which correspond to J magnitudes  $-6.6 < M_J < -6.2$ : as shown in Fig. 3, they populate the upper part of the J region.

Dell'Agli et al. (2014b, 2015a) suggested that the sources of the LMC with the largest IR emission, which populate the reddest regions of the observational planes built with the IRAC Spitzer filters, are the progeny of  $2.5 - 3 M_{\odot}$  stars, and are currently providing the dominant contribution to the overall DPR from the entire galaxy. From the present investigation we deduce that the stars that provide the most relevant contribution to the population of the J region of the LMC are the immediate progenitors of the reddest objects investigated by Dell'Agli et al. (2014b, 2015a).

A significant fraction of the stars in the J region, around 30%, are the progeny of  $1.5 - 1.8 M_{\odot}$  stars formed during the epochs from 1.5 to 2.5 Gyr ago. The surface C/O of these objects is between 1.5 and 2, the DPRs are in the  $2 - 3 \times 10^{-9} M_{\odot}/\text{yr}$  range, with relative contributions from solid carbon and SiC not significantly different from those given above for the higher mass stars. These stars, with luminosities between  $5 \times 10^3 L_{\odot}$  and  $7 \times 10^3 L_{\odot}$ , provide the most relevant contribution to the JLF at  $-6.3 < M_J < -6$  and are mostly located in the fainter side of the J box.

The AGB population of the LMC within the J region also encompasses  $\sim 10\%$  of stars formed around 300 Myr ago from  $\sim 3 M_{\odot}$  progenitors, located in the bright side of the J region (see Fig. 3), where they evolve at luminosities slightly above  $10^4 L_{\odot}$ . Among the sources in the J region these bright stars are those producing dust at the largest rates of  $\sim 5 \times 10^{-9} M_{\odot}/\text{yr}$ .

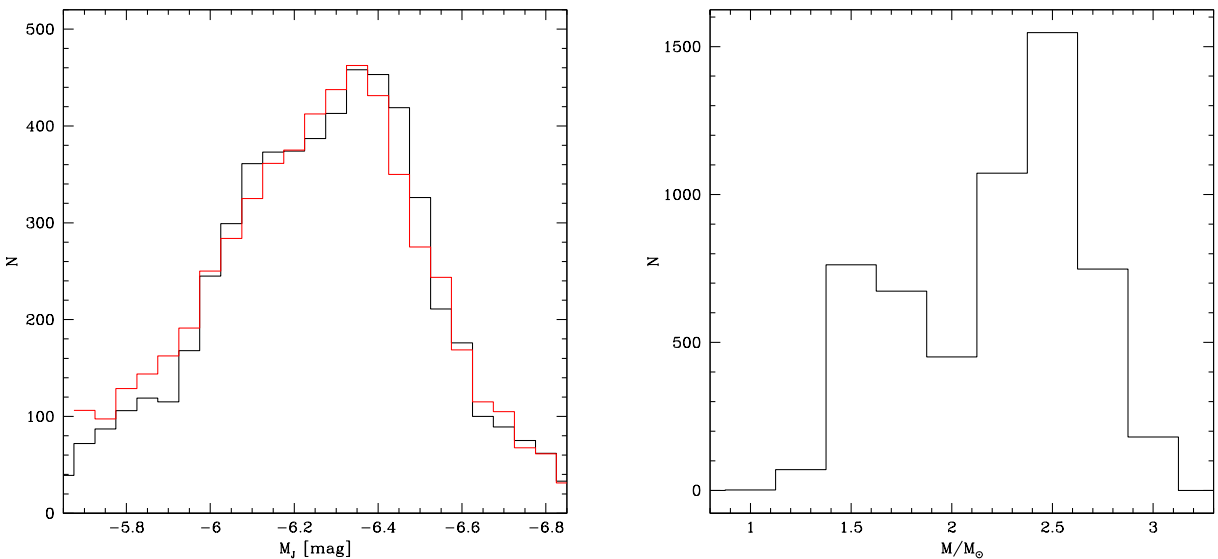


**Fig. 5. Left:** The J luminosity function of the LMC AGB stars populating the J region of the  $(J - K, J)$  plane, obtained by means of population synthesis, is shown in black, and compared with the JLF by Magnus et al. (2024) (red line). **Right:** The distribution of the masses of the stars in the J region of the  $(J - K, J)$  plane, which correspond to the JLF shown in the left panel. The masses of  $M < 1.5 M_{\odot}$  stars refer to the values at the start of the core helium burning phase.

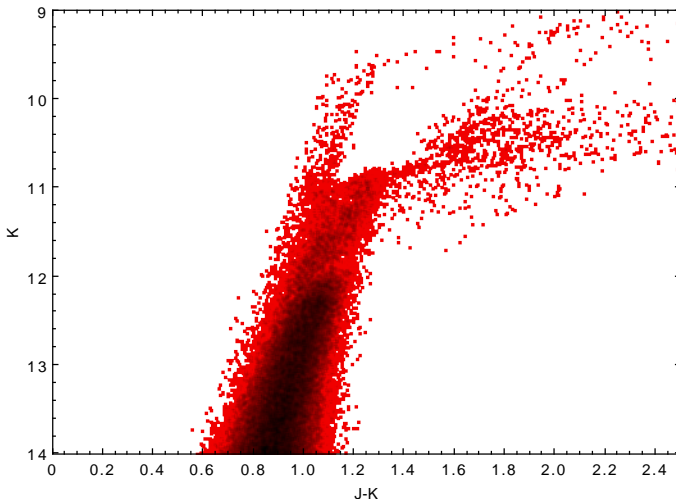


**Fig. 6.** Synthetic distribution of LMC stars evolving through the AGB phase in the colour-magnitude  $(J - K, K)$  plane.

Towards the low luminosity tail of the JLF shown in the left panel of Fig. 5, particularly in the  $M_J > -6$  mag region, we find a group of stars descending from progenitors of mass slightly super solar, which account for  $\sim 2\%$  of the whole population in the J region of the plane. The reason why only a few of these objects are found nowadays in the J region is related to the rapidity with which the evolutionary tracks cross this part of the plane, for the arguments discussed in section 3.4. These are the oldest among the LMC stars considered here, and formed 3-4 Gyr ago.

#### 4.1. The role of the RGB mass loss

According to Mazzi et al. (2021), some star formation took place in the LMC in epochs older than 4 Gyr, when stars of mass below  $\sim 1.2 M_{\odot}$ , now evolving through the AGB, formed. In contrast to their younger and more massive counterparts, the AGB evolution of these stars - specifically their dust-production efficiency

and the resulting displacement of their evolutionary tracks across the observational planes considered - is strongly influenced by  $\delta M_{\text{RGB}}$ , the mass lost during the RGB phase prior to helium-flash ignition. In a recent work on the evolved stellar population of M31, Gavetti et al. (2025) outlined the relevant role of  $\delta M_{\text{RGB}}$  in shaping the luminosity function of the stars of the galaxy populating the blue side of the CMDs obtained with some HST filters, accounting for  $\sim 90\%$  of the entire sample. One of the conclusions drawn by Gavetti et al. (2025) is that for stars of solar or sub-solar mass, RGB mass losses  $\delta M_{\text{RGB}} \sim 0.2 - 0.3 M_{\odot}$  are required to reproduce the observed luminosity function, the detailed value of  $\delta M_{\text{RGB}}$  increasing with metallicity.

As regards the analysis in the present investigation, the choice of  $\delta M_{\text{RGB}}$  is potentially affecting the statistics of the AGB population within the J region, and particularly the last point discussed in the previous sub-section, that the oldest stars now sampled in the J region of the LMC formed  $\sim 4$  Gyr ago. This is because the path towards the formation of carbon stars of low-mass objects depends on the mass of the envelope when the AGB phase begins: in the metal-poor domain, which must be considered if the oldest epochs are taken into account, all the stars that reach the AGB with mass  $M \geq 0.8 M_{\odot}$  become C-stars (Kamath et al. 2023), so that their evolutionary tracks evolve to the red, and thus enter the J region of the CMD. When mass loss during the RGB is considered, the threshold initial mass of the star required to become carbon star is higher than the value given above, which restricts within the J region the mass range of the stars potentially able to evolve.

As stated in section 2, in the analysis developed here we considered the results by Gavetti et al. (2025) and assumed  $\delta M_{\text{RGB}} = 0.2 M_{\odot}$  for all the stars of initial mass  $M < 1.5 M_{\odot}$ . This choice rules out the possibility that these objects, which on the basis of the SFH adopted we estimate to account for  $\sim 30\%$  of the AGB population of the LMC, form carbon dust and evolve to the red side of the CMD, and leads to the conclusion that only the stars younger than 4 Gyr ago must be considered for the statistical analysis of the J region.

To understand the potential impact of  $\delta M_{\text{RGB}}$  on the synthetic JLF of the LMC, we ran numerical simulations based on the as-

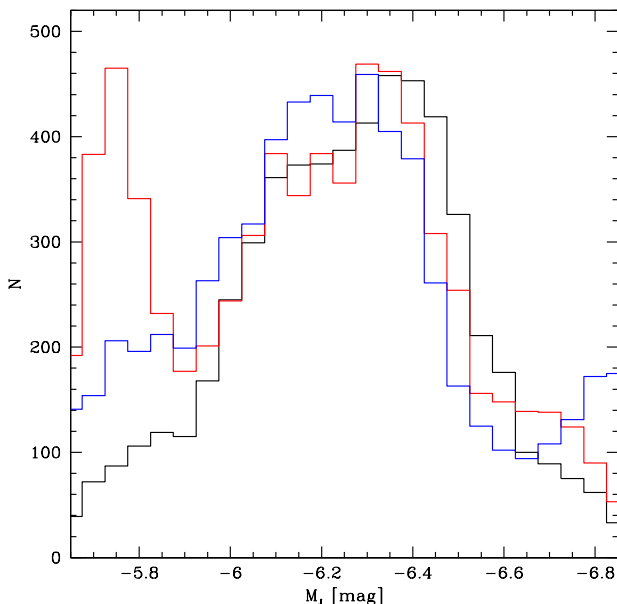


**Fig. 7.** The J luminosity function of the stars in the J region of the LMC, derived on the bases of the assumptions discussed in section 2 (black line), is compared with the results obtained when the metallicity of the stars is artificially kept to  $Z = 10^{-3}$  until presently (blue line) and when RGB mass loss is neglected (red).

sumption that no mass loss occurred during the RGB evolution. The results, shown in Fig. 7, indicate that in this case the JLF would exhibit a low-luminosity peak, whose height is comparable to, though lower than, the main peak discussed above. While the  $\delta M_{\text{RGB}} = 0$  assumption is not realistic, we deduce that a minimum RGB mass loss is required to reproduce the results by Magnus et al. (2024), and that these findings are consistent with those by Gavetti et al. (2025).

#### 4.2. The role of the metallicity enrichment

The study by Carrera et al. (2008) shows that LMC stars have a mean metallicity of  $[\text{Fe}/\text{H}] = -0.5$  and that the stars younger than 3 Gyr formed with  $[\text{Fe}/\text{H}] > -0.5$ . Based on the discussion presented earlier in this section, we know that these slightly sub-solar chemistries characterise the stars within the J region of the CMD, of interest here.

We checked the role played by the chosen AMR, by repeating the population synthesis simulation, assuming that the metallicity of the stars is left unchanged with time and is kept at  $Z = 10^{-3}$  until the present epoch. This experiment is not only intended to test the uncertainties related to the assumed AMR, but also, in a future perspective, to understand which situation must be expected when metal-poor galaxies will be considered.

The results obtained are shown in Fig. 7, where the derived JLF (blue line) is compared with the JLF discussed in the first part of this section (reported in black), which reproduces the results by Magnus et al. (2024). While we note some similarities, particularly in the location of the peak at  $M_J \sim -6.3$  mag and in the morphology of the distribution on the bright side, we also detect some differences that concern the faint side, where the "metal-poor" JLF is significantly flatter than that based on the AMR by Carrera et al. (2008). This result, apparently in contrast with the general idea that metal-poor stars evolve at higher luminosities than the lower metallicity counterparts of the same mass, is explained by the fact that metal-poor stars become car-

bon stars more easily (Kamath et al. 2023), owing to the lower initial oxygen content. As regards the case discussed here, we find that when the low metallicities are adopted, the stars of mass  $\sim 1.5 M_{\odot}$  reach the C-star stage in a less advanced AGB phase than their higher metallicity counterparts of the same mass, thus they spend a longer time within the J box, so their behaviour is more similar to that of the higher mass counterparts discussed in section 3.4. These stars are responsible for the bump in the JLF in the  $-6.2 < M_J < -6.1$  range, seen in Fig. 7. A further difference introduced by the assumption that the stellar population of the LMC is metal-poor is found in the low luminosity tail of the JLF, at  $M_J \sim -5.8$  mag. This is due to the presence of low mass ( $1 - 1.3 M_{\odot}$ ) stars, which in the previous simulation barely entered the J box, while in the present case, due to the easier modality with which they become C-stars, provide a significant contribution to the population on the faint side of the box identifying the J region of the CMD.

## 5. A comparative analysis of the SMC versus the LMC

The same approach based on population synthesis used for the study of the LMC was applied to investigate the J population of the SMC and compare the synthetic JLF with that given in Magnus et al. (2024). As discussed in section 2, in this case we adopted the SFH and the AMR given in Rubele et al. (2018).

The star formation process in the two galaxies proceeded with different modalities. First, the metal enrichment in the LMC was more efficient than in the SMC, which reflects in a lower average  $[\text{Fe}/\text{H}]$  for the latter galaxy, which affects in particular the stellar population formed over the last 2 Gyr. Furthermore, while the SFH of the LMC is characterised by the two peaks mentioned earlier in this section, which occurred 800 Myr and 1.5 Gyr ago, in the SMC there was a single period of intense activity between 4 Gyr and 6 Gyr ago, when the rate of star formation was about a factor of 2 higher than that experienced between 300 Myr and 2 Gyr ago (Rubele et al. 2018). Because of these dissimilarities between the histories of the two galaxies, the stellar populations nowadays evolving along the AGB are significantly different: the AGB population of the SMC is dominated by stars descending from  $1 - 1.5 M_{\odot}$  progenitors, formed during the times running from 6 Gyr ago to 2 Gyr ago, while for the LMC we underlined that the majority of the AGB stars descend from  $1.5 - 1.8 M_{\odot}$  stars formed 1-2 Gyr ago. It is important to understand if and how these differences affect the stellar population of the two galaxies in the J region of the CMD.

Fig. 8 shows the comparison between the JLF obtained for the SMC, indicated with the solid black line, and the corresponding distribution obtained for the LMC, discussed earlier in this section, reported in grey. The JLF of the SMC was artificially scaled to ease the comparison between the two distributions. The first clear difference between the JLF of the two galaxies is the location of the peak, which is almost 0.2 mag fainter in the SMC than in the LMC. This is not surprising, considering that the peak of the JLF at  $M_J = -6.35$  mag of the LMC was determined by the presence of a large number of stars descending from  $\sim 2.5 M_{\odot}$  progenitors; conversely, the peak in the JLF of the SMC, located at  $M_J = -6.15$  mag, is due to the progeny of  $1.2 - 1.8 M_{\odot}$  stars, which are generally fainter than the  $2.5 M_{\odot}$  stars populating the J region of the LMC (see Fig. 3).

Not only the peak, but the whole JLF of the SMC is shifted towards smaller J fluxes in comparison to the LMC, owing to the smaller mass of the progenitors populating the AGB of the

SMC stars with respect to the LMC, and more specifically the J region of the CMD: while in the LMC, as shown in the right panel of Fig. 5, we find that the sources populating the J region are mainly  $2 M_{\odot} < M < 3 M_{\odot}$  stars, the mass distribution of the SMC is more homogeneous, with a majority presence of  $1 M_{\odot} < M < 1.5 M_{\odot}$  objects. The presence of such a significant fraction of low-mass stars is also the reason for the presence of the low luminosity tail in the  $-5.9 < M_J < -5.7$  mag range of the JLF, which can be seen in Fig. 8.

The comparison between the JLF obtained by means of population synthesis and the results from Magnus et al. (2024) are less straightforward and indicative than for the LMC, given the low number of sources on which the statistical analysis by Magnus et al. (2024) is based. The JLF reported in Fig. 8 is similar to the one shown in Fig. F3 by Magnus et al. (2024) for what concerns the location of the peak and the general shape of the JLF on the bright side of the distribution. Differences are found on the faint side of the JLF, mainly because of the aforementioned low luminosity tail, which is not so evident in the results by Magnus et al. (2024). This tail is also the reason for the difference in the average J magnitude, which is found to be  $M_J = -6.1$  mag in the present analysis, whereas Magnus et al. (2024) find  $M_J = -6.18$  mag.

The tail on the faint side of the synthetic distribution is due to the presence of a population of old, metal-poor stars in the J region of the SMC, which descend from progenitors of mass slightly above solar. The possibility that these stars enter the J region is tightly linked to the mass lost during the RGB,  $\delta M_{\text{RGB}}$ : significant RGB mass loss reduces the mass with which the stars start the AGB, so that they undergo an evolutionary path similar to that of the stars belonging to the group I) discussed in section 3.3, with no chance of populating the J region of the plane. The results discussed above, reported with the black, solid line in Fig. 8, were obtained with a mass loss  $\delta M_{\text{RGB}} = 0.2 M_{\odot}$  for stars of mass below  $M = 1.5 M_{\odot}$ . If we assume  $\delta M_{\text{RGB}} = 0.3 M_{\odot}$  for all  $M < 1.5 M_{\odot}$  stars, we obtain the JLF indicated with the red, dashed line in Fig. 8. This is in a much better agreement with the results by Magnus et al. (2024), as also confirmed by the derived average J flux, which is  $M_J = -6.16$  mag. The choice of  $\delta M_{\text{RGB}}$  does not significantly affect the location of the peak of the JLF, because the bulk of the population of the J region of the SMC is made up of the progeny of  $1.2 - 1.8 M_{\odot}$  stars, which are touched only marginally by the assumption of  $\delta M_{\text{RGB}}$ , except for the smaller masses in the mass interval. In a more general context, the results by Freedman & Madore (2020) and Lee et al. (2024a,b) seem to rule out the presence of low luminosity tails in the JLF of all the galaxies investigated: this suggests that significant mass loss occurred during the RGB phase of low mass stars, in agreement with the conclusions given above.

The issue of the mass loss experienced by the stars during the RGB phase is much more relevant for the SMC than for the LMC, because the SMC hosts a much higher fraction of low-mass stars, whose AGB evolution is extremely sensitive to the assumed  $\delta M_{\text{RGB}}$ , which inevitably reflects on the statistics of the masses and luminosities of the population of the J region. The smaller metallicity of SMC stars is a further motivation to take particular care of the mass loss process during the RGB, because metal-poor stars reach the C-star stage more easily, thus it is more likely that they eventually enter the J region.

The present analysis on the properties of the JLF, although limited to only two galaxies, is quite exhaustive, because the LMC and the SMC likely represent the two extreme cases that can occur, at least as far as the peaks of the distribution are concerned. It is hard to think that there could be galaxies whose JLF

peaks brighter than the LMC, i.e.  $-6.35$  mag, which we have seen to correspond to the average J magnitude of  $\sim 2.5 M_{\odot}$  stars, when they evolve within the J region. A brighter peak would demand a dominant population of stars of  $3 M_{\odot}$  or more, which is hard to believe, even if intense star formation occurred during the epochs younger than 300 Myr: indeed the AGB evolutionary time scales drop significantly in the  $M > 2.5 M_{\odot}$  mass domain, and the  $M_J$  vs mass relationship becomes steeper and steeper in that mass range. This conclusion holds even more if the choice recommended by Magnus et al. (2024) to identify the J region is adopted, since  $M > 3 M_{\odot}$  stars are not expected to populate the J region, as shown in Fig. 3.

The SMC represents the opposite extreme case, in that we consider rather unlikely the presence of galaxies whose peak of the JLF is fainter than that of the SMC, i.e.  $-6.15$  mag. Earlier in this section we discussed that the reason for this rather faint peak, at least when compared to the LMC, is the older and lower mass population of the SMC than the LMC, mostly formed around 5 Gyr ago. Even an older burst in the star formation activity would barely change the location of the peak of the JLF, because that would favour the formation of low-mass stars that hardly enter the J region, as they mostly evolve as the stars belonging to the group I) discussed in section 3.3.

Assessing whether the peak J ( $M_J^{\text{peak}}$ ) or rather the average J magnitude ( $M_J^{\text{av}}$ ) of the stars located in the J region of the plane should be used as distance indicator is not an easy task, at least on the basis of the present results, which are restricted to two galaxies only. Use of the  $M_J^{\text{peak}}$  has the advantage that the attention can be focused on a narrow range of masses (hence formation epochs), with a strong bias towards the stars formed around 1 Gyr ago. With the exception of those cases where a burst of star formation occurred 4 Gyr ago (which is the case for the SMC), we expect to find  $M_J^{\text{peak}} \sim -6.3$  mag. On the other hand, the average J magnitude is less sensitive to the details of the SFH between 800 Myr and 4 Gyr ago, as it is affected by the J fluxes of a wider range of stellar masses, whose evolutionary tracks enter the J region. The differences arising from variation in the SFH are softened in this case, as confirmed by the similarity between the values found for the LMC and SMC, which are much closer ( $\delta M_J^{\text{av}} \sim 0.07$  mag) than the corresponding peak magnitudes ( $\delta M_J^{\text{peak}} \sim 0.2$  mag). The shortcoming of the use of  $M_J^{\text{av}}$  is that the results are affected by the uncertainties connected to the modelling of the low mass stars, whose presence has practically no influence on the determination of the peak value. By adopting the average J magnitude one is forced to come across the issues of the treatment of mass loss along the RGB, a physical mechanism highly uncertain, but with a generally strong impact on the statistics for the AGB population of galaxies (Gavetti et al. 2025).

## 6. Conclusions

We use a population synthesis approach to investigate the distribution of MCs AGB stars that occupy the so-called J region of the  $(J - K, J)$  colour-magnitude diagram. This analysis is stimulated by recent studies suggesting that the J-band luminosity function of stars in that region of the plane may serve as distance indicators of galaxies.

Based on the morphology of the evolutionary tracks of stars of various mass and chemical composition on the  $(J - K, J)$  plane, we find that the J population of the galaxies descend from  $1 - 3 M_{\odot}$  stars, between 300 Myr and 5 Gyr old, caught in the evolutionary phases between the stage when they become carbon

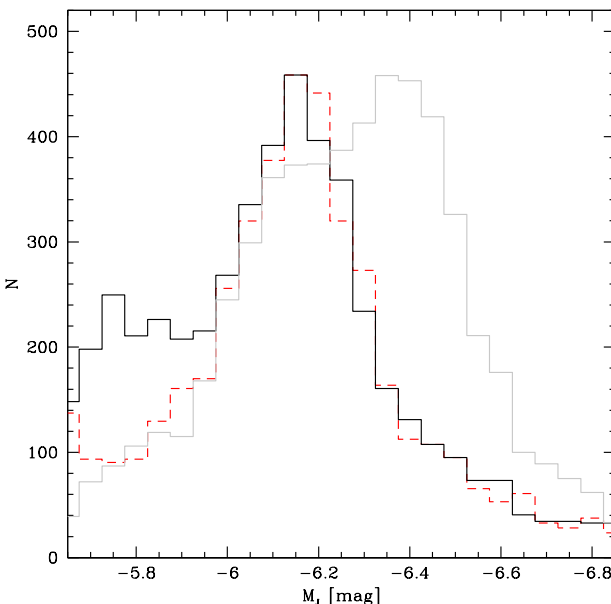


**Fig. 8.** The comparison between the J luminosity functions obtained for the LMC (grey line) and the SMC (black). The red, dashed line indicates the results obtained for the SMC on the basis of the assumption that  $1 - 1.3 M_{\odot}$  metal-poor stars experience a  $0.3 M_{\odot}$  mass loss during the RGB evolution.

stars and the phase when the surface  $C/O \sim 3$ , the latter condition favouring a significant shift of the SED to the IR spectral region, so that the stars evolve off the J region.

The timing of the transit of stars through the J region is extremely sensitive to the mass of the star: while  $M > 2 M_{\odot}$  stars remain in that zone of the plane for a series of 5-6 inter-pulse phases, for a total duration slightly shorter than 1 Myr, the lower-mass counterparts evolve faster, and rapidly evolve to the red side of the plane. In light of this, we expect that in several galaxies the J luminosity function of the stars populating the J region peaks at  $M_J \sim -6.3$  mag, which is the J magnitude of  $2.5 M_{\odot}$  stars during the evolution in that part of the CMD.

The results concerning the LMC are satisfactory and confirm the conclusion given above. The simulation obtained by applying the population synthesis method is fully consistent with the observational scenario, as both the peak of the distribution, found at  $M_J \sim -6.35$  mag, and the width of the J luminosity function on both sides of the peak, are nicely reproduced. Mass loss during the RGB evolution of the order of  $0.2 M_{\odot}$ , in full agreement with previous investigations, must be invoked to prevent the appearance of an unobserved extended tail on the faint side of the J luminosity function.

The J luminosity function of the SMC is shifted to higher  $M_J$ 's than the LMC, the main peak being located at  $M_J \sim -6.15$  mag. We interpret this difference as due to the intense star formation that occurred in the SMC around 5 Gyr ago, when stars of mass slightly above solar formed and are now evolving along the AGB. Under these specific conditions these stars outnumber the  $2 - 3 M_{\odot}$  counterparts, so the peak of the distribution of the J magnitudes occurs at fainter J fluxes than in the LMC. Given the dominant contribution from low-mass stars, in this case the treatment of the RGB mass loss is more relevant than for the LMC. While the expected location of the peak is essentially independent of the amount of mass lost by the stars while climbing along the RGB, to reproduce the faint side of the luminosity function and to derive an average J magnitude  $M_J \sim -6.18$  mag, in agree-

ment with the observations, it is necessary to assume that stars with mass in the  $1 - 1.3 M_{\odot}$  range lose  $0.3 M_{\odot}$  before reaching the TRGB.

*Acknowledgements.* CV and PV acknowledge support by the INAF-Theory-GRANT 2022 “Understanding mass loss and dust production from evolved stars”.

## References

Abel, N. P., van Hoof, P. A. M., Shaw, G., et al. 2008, ApJ, 686, 1125  
 Aller, L. H. & Czyzak, S. J. 1983, ApJS, 51, 211  
 Aringer, B., Girardi, L., Nowotny, W., et al. 2009, A&A, 503, 913  
 Aringer, B., Girardi, L., Nowotny, W., Marigo, P., Bressan, A., 2016, MNRAS, 457, 3611  
 Begemann, B., Dorschner, J., Henning, T., et al. 1994, ApJ, 423, L71  
 Blöcker, T. & Schönberner, D. 1991, A&A, 244, L43  
 Blöcker, T. 1995, A&A, 297, 727  
 Bowen, G. H. 1988, ApJ, 329, 299  
 Boyer, M. L., Srinivasan, S., van Loon, J. T., McDonald, I., Meixner, M., Zaritsky, D., Gordon, K. D., et al., 2011, AJ, 142, 103.  
 Boyer, M. L., Srinivasan, S., Riebel, D., et al. 2012, ApJ, 748, 40  
 Boyer, M. L., Girardi, L., Marigo, P., Williams, B. F., Aringer, B., Nowotny, W., Rosenfield, P., et al., 2013, ApJ, 774, 83.  
 Boyer, M. L., McQuinn, K. B. W., Groenewegen, M. A. T., et al. 2017, ApJ, 851, 152  
 Boyer, M. L., Williams, B. F., Aringer, B., et al. 2019, ApJ, 879, 109  
 Bortolini, G., Östlin, G., Habel, N., Hirschauer, A. S., Jones, O. C., Justtanont, K., Meixner, M., et al., 2024, A&A, 689, A146.  
 Bortolini, G., Correnti, M., Adamo, A., Cignoni, M., Sacchi, E., Tosi, M., Östlin, G., et al., 2025, ApJ, 991, 212.  
 Caloi, V. & D'Antona, F. 2005, A&A, 435, 987  
 Canuto, V. M. C., Mazzitelli, I., 1991, ApJ, 370, 295  
 Carrera, R., Gallart, C., Hardy, E., et al. 2008, AJ, 135, 3, 836  
 Correnti, M., Bortolini, G., Dell'Agli, F., Adamo, A., Cignoni, M., Sacchi, E., Tosi, M., et al., 2025, ApJ, 990, 72.  
 Dell'Agli, F., García-Hernández, D. A., Rossi, C., et al. 2014a, MNRAS, 441, 1115.  
 Dell'Agli, F., Ventura, P., García Hernández, D. A., et al. 2014b, MNRAS, 442, L38  
 Dell'Agli, F., Ventura, P., Schneider, R., et al. 2015a, MNRAS, 447, 2992  
 Dell'Agli, F., García-Hernández, D. A., Ventura, P., et al. 2015b, MNRAS, 454, 4235  
 Dell'Agli, F., Di Criscienzo, M., Boyer, M. L., et al. 2016, MNRAS, 460, 4230  
 Dell'Agli, F., Di Criscienzo, M., Ventura, P., et al. 2018, MNRAS, 479, 5035  
 Dell'Agli, F., Di Criscienzo, M., García-Hernández, D. A., et al. 2019, MNRAS, 482, 4733  
 Di Criscienzo, M., Tailo, M., Milone, A. P., et al. 2015, MNRAS, 446, 1469  
 Ferrarotti, A. S. & Gail, H.-P. 2001, A&A, 371, 133  
 Ferrarotti, A. S. & Gail, H.-P. 2002, A&A, 382, 256  
 Ferrarotti, A. S. & Gail, H.-P. 2006, A&A, 447, 553  
 Freedman, W. L. & Madore, B. F. 2020, ApJ, 899, 1, 67  
 Freedman, W. L., Madore, B. F., Hoyt, T. J., Jang, I. S., Lee, A. J., Owens, K. A., 2025, ApJ, 985, 203.  
 Gail, H.-P. & Sedlmayr, E. 1985, A&A, 148, 183  
 Gavetti, C., Ventura, P., Dell'Agli, F., et al. 2025, A&A, 699, A23  
 Goldman, S. R., van Loon, J. T., Zijlstra, A. A., et al. 2017, MNRAS, 465, 403  
 Goldman, S. R., Boyer, M. L., Dalcanton, J., et al. 2022, ApJS, 259, 41, G22  
 Groenewegen, M. A. T. & Sloan, G. C. 2018, A&A, 609, A114  
 Habing, H. J., 1996, A&ARv, 7, 97.  
 Harris, J., Zaritsky, D., 2009, AJ, 138, 1243.  
 Hauschildt, P. H., Allard, F., Ferguson, J., et al. 1999, ApJ, 525, 871  
 Höfner, S. & Olofsson, H. 2018, A&A Rev., 26, 1  
 Iben, I. Jr. 1974, ARA&A, 12, 215  
 Kamath, D., Dell'Agli, F., Ventura, P., et al. 2023, MNRAS, 519, 2169  
 Karakas, A. I., Lattanzio, J. C. 2014, PASA, 31, e030  
 Kobayashi, C., Karakas, A. I., & Lugaro, M. 2020, ApJ, 900, 179  
 Kroupa, P. 2001, MNRAS, 322, 231.  
 Laor, A. & Draine, B. T. 1993, ApJ, 402, 441.  
 Lee, A. J., Freedman, W. L., Jang, I. S., Madore, B. F., Owens, K. A., 2024, ApJ, 961, 132.  
 Lee, A. J., Weisz, D. R., Ren, Y., et al. 2024, arXiv:2410.09256.  
 Lewis, A. R., Dolphin, A. E., Dalcanton, J. J., et al. 2015, ApJ, 805, 183  
 Li, S., Riess, A. G., Scolnic, D., Casertano, S., Anand, G. S., 2025, ApJ, 988, 97.  
 Madore, B. F. & Freedman, W. L. 2020, ApJ, 899, 1, 66  
 Magnus, E., Groenewegen, M. A. T., Girardi, L., et al. 2024, A&A, 691, A350  
 Marigo, P. 2002, A&A, 387, 507  
 Marigo, P., Girardi, L., & Chiosi, C. 2003, A&A, 403, 225

Marigo, P. & Aringer, B. 2009, A&A, 508, 1539

Marini, E., Dell'Agli, F., Di Criscienzo, M., et al. 2020, MNRAS, 493, 2996

Marini, E., Dell'Agli, F., Groenewegen, M. A. T., et al. 2021, A&A, 647, A69

Marini, E., Dell'Agli, F., Kamath, D., Ventura, P., Mattsson, L., Marchetti, T., García-Hernández, D. A., et al., 2023, A&A, 670, A97

Matsuura, M., Barlow, M. J., Zijlstra, A. A., et al. 2009, MNRAS, 396, 918

Matsuura, M. 2011, Why Galaxies Care about AGB Stars II: Shining Examples and Common Inhabitants, 445, 531

Matsuura, M., Woods, P. M., & Owen, P. J. 2013, MNRAS, 429, 2527.

Mazzi, A., Girardi, L., Zaggia, S., et al. 2021, MNRAS, 508, 1, 245

Miglio, A., Chiappini, C., Mackereth, J. T., et al. 2021, A&A, 645, A85

Nanni, A., Bressan, A., Marigo, P., et al. 2013, MNRAS, 434, 2390

Nanni, A., Bressan, A., Marigo, P., et al. 2014, MNRAS, 438, 2328

Nanni, A., Marigo, P., Groenewegen, M. A. T., et al. 2016, MNRAS, 462, 1215

Nanni, A., Groenewegen, M. A. T., Aringer, B., et al. 2019, MNRAS, 487, 502

Nenkova, M., Ivezic, Z., & Elitzur, M. 1999, Thermal Emission Spectroscopy and Analysis of Dust, Disks, and Regoliths, 20

Nikolaev, S. & Weinberg, M. D. 2000, ApJ, 542, 2, 804

Paczyński, B. 1970, Acta Astron., 20, 47

Reimers, D. 1975, Memoires of the Societe Royale des Sciences de Liege, 8, 369

Ripoche, P., Heyl, J., Parada, J., et al. 2020, MNRAS, 495, 3, 2858

Romano, D. 2022, A&A Rev., 30, 1, 7

Rouleau, F. & Martin, P. G. 1991, ApJ, 377, 526.

Rubele, S., Pastorelli, G., Girardi, L., et al. 2018, MNRAS, 478, 4, 5017

Sackmann, I.-J. & Boothroyd, A. I. 1992, ApJ, 392, L71. doi:10.1086/186428

Salaris, M. 2012, Red Giants as Probes of the Structure and Evolution of the Milky Way, 26, 45

Salaris, M., Cassisi, S., & Pietrinferni, A. 2016, A&A, 590, A64

Salaris, M., Cassisi, S., Schiavon, R. P., et al. 2018, A&A, 612, A68

Schneider, R., Valiante, R., Ventura, P., et al. 2014, MNRAS, 442, 1440

Schlegel, D. J., Finkbeiner, D. P., Davis, M., 1998, ApJ, 500, 525.

Schneider, R., Maiolino, R., 2023, arXiv, arXiv:2310.00053

Schröder, K.-P. & Cuntz, M. 2005, ApJ, 630, L73

Schwarzschild, M. & Härm, R. 1965, ApJ, 142, 855

Sloan, G. C., Matsuura, M., Lagadec, E., et al. 2012, ApJ, 752, 140

Sloan, G. C., Lagadec, E., Zijlstra, A. A., et al. 2014, ApJ, 791, 28

Sloan, G. C., Kraemer, K. E., McDonald, I., et al. 2016, ApJ, 826, 44

Srinivasan, S., Boyer, M. L., Kemper, F., et al. 2016, MNRAS, 457, 2814

Tailo, M., Di Criscienzo, M., D'Antona, F., et al. 2016, MNRAS, 457, 4525

Tailo, M., Milone, A. P., Lagioia, E. P., et al. 2021, MNRAS, 503, 694

VandenBerg, D. A. & Denissenkov, P. A. 2018, ApJ, 862, 72

van Loon, J. T. 2000, A&A, 354, 125

van Loon, J. T., Marshall, J. R., Zijlstra, A. A. 2005, A&A, 442, 597

Vassiliadis, E. & Wood, P. R. 1993, ApJ, 413, 641, VW93

Ventura, P., Zeppieri, A., Mazzitelli, I., D'Antona, F., 1998, A&A, 334, 953

Ventura, P., D'Antona, F., Mazzitelli, I., et al. 2001, ApJ, 550, L65.

Ventura, P., D'Antona, F. 2005, A&A, 431, 279

Ventura, P. & Marigo, P. 2009, MNRAS, 399, L54

Ventura, P. & Marigo, P. 2010, MNRAS, 408, 2476

Ventura, P., Di Criscienzo, M., Schneider, R., et al. 2012, MNRAS, 420, 1442

Ventura, P., Di Criscienzo, M., Carini, R., et al. 2013, MNRAS, 431, 3642

Ventura, P., Dell'Agli, F., Schneider, R., et al. 2014, MNRAS, 439, 977

Ventura, P., Karakas, A., Dell'Agli, F., et al. 2018, MNRAS, 475, 2282.

Ventura, P., Dell'Agli, F., Tailo, M., et al. 2022, Universe, 8, 45.

Vincenzo, F., Belfiore, F., Maiolino, R., et al. 2016, MNRAS, 458, 3466

Vitense, E. 1953, ZAp, 32, 135

Wachter, A., Schröder, K.-P., Winters, J. M., et al. 2002, A&A, 384, 452

Wachter, A., Winters, J. M., Schröder, K.-P., et al. 2008, A&A, 486, 497

Weinberg, M. D. & Nikolaev, S. 2001, ApJ, 548, 2, 712

Williams, B. F., Dolphin, A. E., Dalcanton, J. J., et al. 2017, ApJ, 846, 145